IIETA International Information and Engineering Technology Association
Advancing the World of Information and Engineering

Journal Européen des Systèmes Automatisés
Vol. 59, No. 4, April, 2026, pp. 1061-1068
Journal homepage: http://iieta.org/journals/jesa

Wettability, Surface Morphology, and Wet Flashover Response of SiO_2-Graphene-Coated 150 kV Ceramic Insulators Under Natural Contamination

Yusreni Warmi[1*], Nofriady Handra[1], Taufal Hidayat[1], Agus Sukarto Wismogroho[2], Martini Martini[1], Muhammad Naufalunn Nabil[3]

[1] Department of Electrical Engineering, Faculty of Engineering, Institut Teknologi Padang, Padang 25143, Indonesia
[2] National Research and Innovation Agency (BRIN), Jakarta 10340, Indonesia
[3] Department of Mechanical Engineering, Faculty of Engineering, Universitas Andalas, Padang 25163, Indonesia

Corresponding Author Email: yusreni@itp.ac.id

https://doi.org/10.18280/jesa.590416

Received: 5 February 2026
Revised: 1 April 2026
Accepted: 11 April 2026
Available online: 30 April 2026

Keywords:
ceramic insulator, SiO_2-graphene coating, natural contamination, hydrophobicity, contact angle, leakage current, wet flashover, surface morphology

ABSTRACT

This work examines SiO_2, graphene, and SiO_2-graphene coatings on naturally contaminated 150 kV ceramic insulators by combining static contact-angle measurement, FE-SEM/EDS observation, FTIR spectra, wet flashover testing, and leakage-current measurement. The SiO_2 system increased the contact angle from 72.57 ± 24.59° to 110.58 ± 3.09°, graphene from 56.73 ± 7.31° to 101.79 ± 3.44°, and the SiO_2-graphene system from 21.32 ± 2.71° to 105.88 ± 1.95°. For the hybrid surface, EDS also showed the appearance of carbon (13.45 mass%) together with a higher silicon fraction (26.65 mass%), which supports successful surface deposition. Although the wettability improvement was clear, the wet flashover voltage of the hybrid-coated insulators decreased by 9.8% in the DF4 series and by 24.3% in the L3 series, while leakage current at moderate stress remained low (0.014-0.020 mA). These results indicate that static hydrophobicity alone is not enough to predict wet flashover performance under biological contamination. The most plausible explanation is that moisture-retaining deposits, local coating non-uniformity, and defect-assisted conductive wet paths still govern discharge initiation. The discussion therefore, separates direct observations from probable mechanisms and avoids overstating morphology-chemistry coupling beyond the available evidence.

1. INTRODUCTION

Outdoor high-voltage insulators are essential components in power transmission systems because they maintain electrical insulation while mechanically supporting energized conductors. However, the long-term reliability of these components is strongly influenced by environmental exposure, particularly surface contamination and moisture accumulation. Under polluted and humid conditions, contaminants deposited on insulator surfaces can interact with moisture to form conductive films that increase leakage current and may eventually initiate surface flashover [1, 2]. In tropical environments, biological contaminants such as moss, algae, and organic deposits are frequently observed on ceramic insulators. These biological pollutants can retain moisture for extended periods, intensify surface conductivity, and increase the probability of electrical discharge initiation.

Surface wettability plays a key role in determining the electrical behavior of outdoor insulation systems. Hydrophilic surfaces tend to promote continuous water-film formation, which facilitates leakage current flow and increases flashover susceptibility under wet conditions, whereas hydrophobic coatings can reduce water spreading and improve surface insulation performance [3-5]. Conventional ceramic insulators inherently exhibit relatively high surface energy and microstructural porosity, making them prone to moisture spreading and contaminant accumulation [1, 2]. Consequently, surface modification techniques have been widely investigated to enhance hydrophobicity and improve the environmental durability of ceramic insulators without altering their intrinsic dielectric properties.

Among the various modification strategies, silica-based coatings have attracted considerable attention because of their chemical stability, adjustable surface morphology, and compatibility with scalable deposition techniques such as spray coating [4]. The incorporation of nanoscale SiO_2 particles can generate micro/nano surface structures that enhance water repellency by suppressing continuous liquid-film formation on the insulator surface. In addition, graphene-based materials have emerged as promising components for functional coatings owing to their two-dimensional morphology, low surface energy, and barrier characteristics, which are beneficial for reducing moisture penetration and surface degradation [6, 7].

Recent studies indicate that hybrid coatings combining inorganic nanoparticles and carbon-based nanomaterials can provide advantages in controlling surface wetting behavior. In such systems, both surface morphology and surface chemistry

are relevant to the stability of hydrophobic performance [6-8]. The effectiveness of hybrid coatings depends not only on surface roughness or chemical composition independently, but also on the interaction between coating morphology and interfacial chemistry. These coatings can modify surface roughness, reduce moisture spreading, and may delay the development of leakage current and dry-band arcing phenomena under contaminated conditions.

Despite these advances, the relationship between coating-induced wettability enhancement and the resulting electrical flashover behavior remains insufficiently understood. Many previous studies primarily emphasize improvements in contact angle or hydrophobic performance, while the electrical response of coated insulators under severe contamination conditions has received comparatively less attention [1, 2, 8]. In particular, natural biological contamination may alter the wetting mechanism by promoting persistent moisture retention and conductive film formation on the insulator surface, thereby influencing the effectiveness of hydrophobic coatings. Since flashover processes are strongly influenced by localized wet-film continuity and electric-field intensification along contaminated surfaces, a deeper understanding of how coating morphology and surface chemistry jointly affect electrical behavior is required.

Against this background, three coating routes (SiO_2, graphene, and hybrid SiO_2-graphene) were evaluated on naturally contaminated 150 kV ceramic insulators by combining contact-angle measurement, FE-SEM/EDS observation, FTIR spectra, wet flashover tests, and leakage-current measurement. Rather than treating hydrophobicity improvement as an automatic proxy for electrical improvement, the analysis compares the surface observations with the actual electrical-test results.

Three research questions guide the analysis: (1) how strongly do the three coatings change the measured contact angle of contaminated ceramic surfaces; (2) do FE-SEM/EDS and FTIR observations support a more compact and chemically modified coated surface, especially for the SiO_2-graphene system; and (3) does higher static hydrophobicity coincide with better wet flashover performance under natural biological contamination? The working hypothesis is that the hybrid coating improves surface wettability and apparent surface coverage, but wet flashover remains controlled by contamination-assisted conductive paths, local non-uniformity, and defect-triggered discharge initiation.

2. METHOD

2.1 Ceramic substrate preparation

Commercial ceramic insulator specimens served as the substrates in this work. Prior to coating application, the ceramic surfaces were cleaned to remove surface contaminants, dust, and residual impurities that could influence wettability measurements and surface-energy conditions. The cleaning step was intended to improve coating adhesion and reduce variability during comparative testing. Uncoated ceramic samples were retained as reference specimens for comparison with the coated surfaces.

The SiO_2-coated specimens (L6/L2) were prepared by exposing the ceramic insulator surfaces to natural dust and moss contamination in order to represent outdoor service-related contamination conditions commonly encountered by high-voltage insulators. Subsequently, a SiO_2 coating was applied using a spray-deposition method. The uncoated and SiO_2-coated specimens are summarized in Table 1.

Table 1. SiO_2-coated insulator specifications

Sample	Coating	Information
Uncoated 	None	Surface exposed to natural dust/moss contamination before coating
SiO_2 Coated 	SiO_2	Surface after SiO_2 coating application for comparative evaluation

Graphene-coated specimens (DM/D3) were prepared following the same general procedure. The ceramic insulator surfaces were first exposed to natural dust contamination and then coated with graphene using the spray method. The uncoated and graphene-coated specimens are summarized in Table 2.

Table 2. Graphene-coated insulator specifications

Sample	Coating	Information
Uncoated 	None	Surface exposed to natural dust contamination before coating
Graphene-coated 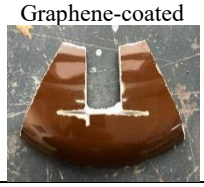	Graphene	Surface after graphene coating application for comparative evaluation

Table 3. SiO_2-graphene composite insulator specifications

Sample	Coating	Information
Uncoated 	None	Surface exposed to natural moss contamination before coating
SiO_2-Graphene Coated 	SiO_2-Graphene	Surface after hybrid coating application for comparative evaluation

The hybrid SiO_2-graphene specimens (LM/L10) were prepared from ceramic insulator surfaces affected by natural moss contamination. After the contamination stage, the hybrid SiO_2–graphene coating was applied using the same general

spray-based workflow. The uncoated and hybrid-coated specimens are summarized in Table 3.

All specimen groups were prepared for the same comparative experimental sequence, consisting of contact-angle measurement, FE-SEM/EDS observation, FTIR characterization, and electrical testing under the available dataset conditions. The surface-pollution and electrical-test interpretation was kept consistent with the general principle that pollution, moisture, and surface conductivity jointly affect insulation performance [9].

2.2 Coating formulation and spray deposition

Three coating systems were evaluated: SiO_2, graphene, and hybrid SiO_2-graphene. Spray deposition was applied consistently across all systems so that the coating method remained comparable among specimens. However, process variables such as nozzle geometry, atomizing pressure, exact stand-off distance, and coating thickness were not instrument-recorded in the archived dataset. For that reason, coating preparation was treated as a controlled comparative step rather than as an independently optimized process variable, and this limitation is stated explicitly.

The purpose of the coating stage was comparative rather than parametric: to assess whether the three deposited surface systems produce different wettability and electrical responses under the same experimental workflow. Engineering recommendations related to spray pressure, solids loading, or thickness optimization are intentionally not claimed from the present dataset.

Within this scope, the hybrid SiO_2-graphene system is interpreted as a morphology-chemistry relationship supported qualitatively by FE-SEM/EDS and FTIR, not as a fully quantified interfacial coupling parameter.

Spray-based coating methods have been widely adopted in both electrical insulation and functional coating studies due to their flexibility and suitability for field-scale implementation, making the present experimental configuration relevant not only for laboratory evaluation but also for practical outdoor insulation applications [3-5].

2.3 Wettability measurement

Surface wettability was evaluated using the sessile-drop method with a 50 μL distilled-water droplet, and the reported angle for each point was taken as the average of the left and right droplet profiles. For each surface condition, three measurement points were recorded ($n = 3$). Descriptive statistics are reported as mean ± standard deviation, and Welch's t-test was used only for before-versus-after contact-angle comparison within each coating system because raw point-wise values were available only for this dataset.

Here, a higher contact angle indicates stronger water repellency, whereas a lower standard deviation indicates better spatial uniformity of the wettability response. This distinction is important because flashover on contaminated insulators is often initiated locally rather than by the surface-average value alone.

Static contact-angle measurement is widely accepted as a practical and reliable indicator of surface hydrophobicity for ceramic insulators and functional coatings, particularly in studies focusing on surface wetting behavior rather than dynamic droplet motion [10-14]. Previous investigations have demonstrated that reduced contact-angle values, enhanced surface conductivity, and localized wet-film continuity can increase susceptibility to leakage current and flashover under humid or polluted conditions [1, 2, 8].

Contact-angle analysis, therefore provides a quantitative basis for evaluating how effectively the SiO_2, graphene, and SiO_2-graphene composite coatings modify surface wettability. This parameter is directly relevant to the electrical performance and environmental durability of outdoor high-voltage insulation systems [3-8].

2.4 Microstructural characterization (FE-SEM)

FE-SEM was used to examine the coated and uncoated surfaces qualitatively, with emphasis on visible porosity, particle agglomeration, coating continuity, and defect distribution. Because no AFM roughness data, particle-size histogram, or image-based porosity quantification were available in the recorded dataset, the FE-SEM discussion is intentionally limited to observable morphological features.

For this reason, descriptors such as 'more continuous' or 'more compact' are used only as qualitative image-supported observations and are not presented as quantified roughness metrics such as Ra or Rq.

In this work, FE-SEM analysis served as a complementary technique to contact-angle measurements by providing qualitative microstructural evidence for the observed wettability trends of SiO_2, graphene, and hybrid SiO_2-graphene composite coatings. Similar approaches combining surface observation and wettability analysis have been widely reported in studies of functional coatings for electrical insulation and superhydrophobic surface engineering [3-5, 12, 13].

2.5 Chemical characterization (FTIR)

FTIR was used as a qualitative chemical indicator for silica-related and carbon-related features after coating. The spectra were not used as stand-alone proof of a specific bond-level coupling such as Si-C. Instead, the FTIR results were interpreted together with EDS composition changes to support successful surface deposition and a modified surface chemical environment after coating. A stronger claim about interfacial bonding would require XPS, peak deconvolution, or other surface-sensitive techniques, which were not part of the present dataset. This limitation is stated explicitly. In hybrid composite systems, FTIR analysis provides qualitative evidence of successful material integration by revealing the coexistence of inorganic and carbon-based functional groups within the same coating matrix. Such coexistence is important for surface modification, where surface chemistry complements microstructural roughness in stabilizing hydrophobic behavior under humid or contaminated conditions [4, 6, 7]. The FTIR results therefore support the interpretation of wettability performance by linking observed contact-angle behavior to chemical features associated with the SiO_2, graphene, and SiO_2-graphene composite coatings. Similar combined use of FTIR spectroscopy and wettability analysis has been reported in studies of functional coatings for dielectric and outdoor insulation applications [3-8].

2.6 Flashover and leakage current testing

Flashover testing was conducted under dry and wet conditions, and leakage current was measured at 50% of the

measured flashover voltage for 10 s as a moderate-stress comparative diagnostic rather than as a universal design standard. Wet flashover values are reported from repeated tests (n = 6), whereas the leakage-current values archived in the manuscript are summarized condition-wise. The discussion therefore avoids unsupported causal claims and clearly separates descriptive electrical results from probable mechanisms.

3. RESULTS AND DISCUSSION

3.1 Wettability performance

The contact-angle results show a consistent upward shift after coating for all three systems, but the magnitude and statistical strength of the change differ among them. For the SiO_2 specimens, the average contact angle increased from 72.57 ± 24.59° to 110.58 ± 3.09°. For graphene, it increased from 56.73 ± 7.31° to 101.79 ± 3.44°. For the hybrid SiO_2-graphene specimens, it increased from 21.32 ± 2.71° to 105.88 ± 1.95°.

The detailed contact-angle data before and after coating are summarized in Table 4, which provides the basis for comparing the wettability improvement among the SiO_2, graphene, and SiO^2-graphene coating systems.

Welch's t-test indicates that the improvement is statistically significant for graphene ($p = 0.0029$) and especially for the hybrid system ($p < 0.001$), whereas the SiO_2-only system shows a strong numerical increase but does not reach $p < 0.05$ ($p = 0.114$) because one pre-coating value remained relatively high and the dataset is small (n = 3 per condition). Thus, the strongest evidence-based statement is that all coatings increase the measured contact angle, while the hybrid surface provides the narrowest post-coating dispersion.

Table 4. Contact angle measurements before and after coating

Coating System	Before CA (°)	After CA (°)	ΔCA (%)	P-Value	Interpretation
SiO_2	72.57 ± 24.59	110.58 ± 3.09	+52.4	0.114	Numerical rise; high pre-coating spread
Graphene	56.73 ± 7.31	101.79 ± 3.44	+79.4	0.0029	Significant increase
SiO_2-Graphene	21.32 ± 2.71	105.88 ± 1.95	+396.7	<0.001	Largest and most uniform increase
ANOVA (after)	-	-	-	0.0278	Post-coating means differ among systems

This is more informative than simply calling the coating 'hydrophobic.' The hybrid system transforms a severely wettable moss-contaminated surface (21.32 ± 2.71°) into a uniformly water-repellent one (105.88 ± 1.95°), which is a much stronger surface-state change than that observed from the SiO_2-only route.

At the same time, these wettability data should not be overextended. Static contact angle captures a local near-surface wetting response under a small droplet, whereas flashover under contaminated wet conditions depends on the continuity of conductive pathways over a much larger stressed surface. For this reason, contact-angle enhancement is not treated as direct proof of improved wet flashover strength.

3.2 FE-SEM analysis of coating morphology

The FE-SEM observations are interpreted qualitatively. The uncoated ceramic surface shows irregular topography, visible pores, and surface defects that are compatible with easier moisture retention. After SiO_2 coating, granular surface features become more apparent, suggesting partial coverage by inorganic particles. The graphene-coated surface shows broader plate-like regions, while the hybrid surface appears more continuously covered with fewer visibly open defective regions.

These observations support an apparent morphological progression from heterogeneous exposed ceramic to a more covered composite-like surface. However, because no roughness measurement, particle-size statistics, or porosity image analysis was performed, terms such as 'hierarchical' and 'more continuous' are now used as qualitative descriptors tied to the SEM images rather than quantified structural metrics.

Practically, this morphological change suggests that the hybrid coating can reduce exposed high-energy ceramic sites and moderate local wetting heterogeneity. That interpretation remains consistent with the narrower post-coating contact-angle dispersion, but it is presented as a surface observation rather than as direct electrical proof. Figure 1 presents the FE-SEM surface morphology and FTIR spectra of the uncoated, SiO_2-coated, and SiO_2-graphene-coated 150 kV ceramic insulators. The figure supports the interpretation that the hybrid coating produces a more continuous surface coverage and provides qualitative evidence of chemical features associated with the coating layer.

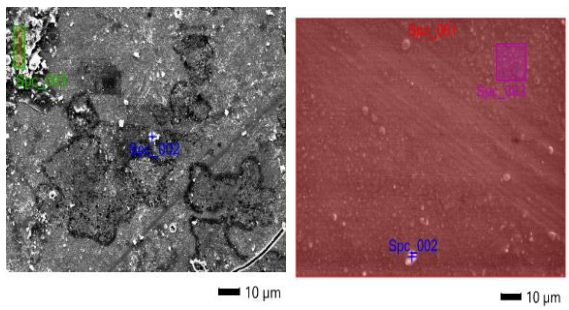

(a) After (b) After

Figure 1. (a, b) FE-SEM surface morphology and FTIR spectra of uncoated, SiO_2-coated, and SiO_2-graphene-coated 150 kV ceramic insulators

3.3 FTIR analysis and chemical interaction

The FTIR spectra are interpreted as qualitative evidence of coating-related chemical features, not as definitive proof of a specific bond architecture. The spectra indicate silica-related absorption bands for the SiO_2-containing coatings and carbon-related features after graphene incorporation.

This interpretation is strengthened when the spectra are read together with the EDS results from the raw experiment file: for the hybrid sample, carbon appears after coating at 13.45 mass% and silicon increases to 26.65 mass%, whereas the uncoated counterpart did not show measurable carbon and contained only 10.73 mass% silicon.

Taken together, the data support successful surface

deposition and a modified surface chemical environment, rather than proving that FTIR alone establishes strong morphology-chemistry coupling.

Overall, the evidence remains convergent but qualitative: FE-SEM indicates a more covered surface, EDS indicates changed elemental composition, and FTIR indicates coating-related functional features, as shown in Figure 2. Figure 2 presents the FTIR spectra of the SiO_2-coated and SiO_2-graphene composite coatings, supporting the qualitative interpretation of silica-related and carbon-related features after coating.

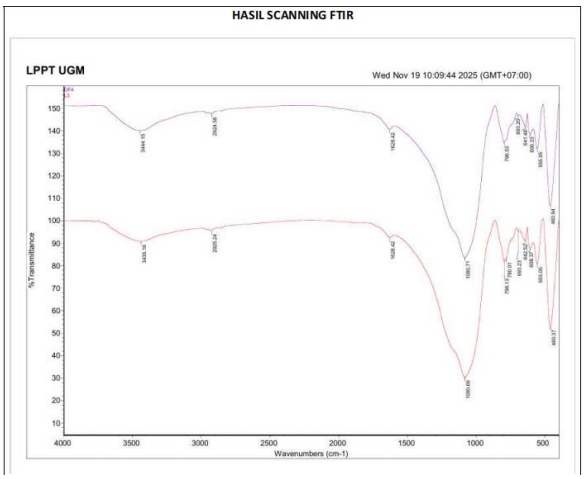

Figure 2. FTIR spectra of SiO_2-coated and SiO_2-graphene composite coatings on 150 kV ceramic insulators

A stronger claim about interfacial bonding would require XPS or additional spectroscopy, which were not part of the present dataset. This limitation is stated explicitly to keep the chemical interpretation fully aligned with the evidence level.

The corresponding elemental composition obtained from EDS analysis is described in the text, while the surface morphology before and after coating is shown in Figure 1.

3.4 Structure property relationship and electrical relevance

Overall, the dataset supports an observed relationship among surface coverage, wettability response, and electrical behavior, but not a fully quantified predictive coupling model. The hybrid coating shows the clearest surface-state improvement in terms of post-coating contact angle and spatial uniformity, and the FE-SEM/EDS/FTIR evidence is consistent with a more effectively modified outer surface.

However, the electrical results show that this surface-state improvement does not automatically suppress wet flashover. The interpretation separates two levels of behavior: (i) local wetting behavior measured by static contact angle and (ii) long-path electrical breakdown behavior controlled by conductive film continuity, field intensification, contamination heterogeneity, and local coating defects.

The main contribution is therefore not only material-based but also interpretive: the dataset shows how a very favorable hydrophobic response can still coincide with weak or even adverse wet flashover outcomes under biological contamination.

This distinction is more precise than simply labeling the hybrid coating as either ‘effective’ or ‘ineffective.’ Thus, the mismatch between surface-state improvement and electrical outcome is treated as the main scientific result, not as a contradiction that should be hidden.

A future predictive model would require thickness-resolved coating characterization, quantified contamination severity, and real-time wet-path diagnostics, none of which were available in the present dataset. Within these limits, the work still provides a useful surface-to-electrical interpretation grounded in the actual measurements. The flashover-voltage and leakage-current responses under dry and wet conditions are summarized in Tables 5 and 6 to clarify the electrical performance of each coating system.

3.5 Electrical performance evaluation

The wet electrical results do not mirror the contact-angle improvement. For the DF4 series, the wet flashover voltage decreased from 15.33 ± 0.40 kV to 13.83 ± 0.38 kV after hybrid coating, corresponding to a 9.8% reduction. For the L3 series, it decreased from 18.50 ± 0.51 kV to 14.00 ± 0.39 kV, corresponding to a 24.3% reduction. By contrast, the available leakage-current readings at moderate stress remain low, within 0.014-0.020 mA.

These results support a cautious conclusion: under the present natural-contamination conditions, improved static hydrophobicity did not translate into higher wet flashover voltage. The most plausible explanation is that moisture-retaining biological deposits, together with local coating non-uniformity or defect sites, still maintained electrically continuous wet paths that dominated breakdown initiation. This interpretation is consistent with prior work showing that surface wetting, contamination, and coating durability can strongly influence leakage-current and flashover behavior [1, 2, 8, 15, 16]. urther studies on coated and contaminated insulators similarly indicate that coating damage, contamination distribution, and leakage-current features must be considered when interpreting flashover behavior and insulator condition [17-20]. More recent studies on hydrophobic surface-energy control, nano-TiO_2 coatings, porcelain-insulator coating performance, and condensation-related flashover behavior also emphasize that coating chemistry, surface energy, and moisture dynamics can affect leakage current and flashover resistance [21-25].

Other explanations are also possible. Besides contamination-assisted conductive films, the flashover decrease may also be influenced by local thickness non-uniformity, imperfect coating adhesion, or changes in surface resistance under high-field wet conditions. Figure 3 compares the wet flashover voltage before and after SiO_2-graphene coating, while Table 5 summarizes the dry and wet flashover-voltage data.

Table 5. Flashover voltage comparison (Dry and Wet conditions)

Condition	Dry Flashover (kV)	Wet Flashover (kV, Mean ± SD)	Change vs. Uncoated
Uncoated (Before DF4)	30	15.33 ± 0.40	-
Hybrid-coated (DF4)	31	13.83 ± 0.38	-9.8%
Uncoated (Before L3)	36	18.50 ± 0.51	-
Hybrid-coated (L3)	32	14.00 ± 0.39	-24.3%

Table 6. Leakage current at 50% flashover voltage

Condition	Test Voltage (kV)	Leakage Current (mA)
Before DF4	19	0.016
DF4 Coating 1	18	0.020
Before L3	18	0.014
L3 Coating 1	18	0.014

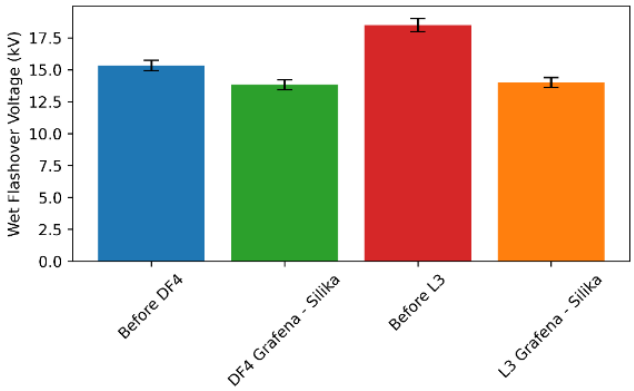

Figure 3. Comparison of wet flashover voltage of ceramic insulators before and after SiO_2-graphene coating

Because the complete raw replicate series for flashover and leakage current are not preserved in the manuscript archive, these electrical results are discussed descriptively rather than inferentially. Figure 4 presents the leakage-current response measured at 50% of the flashover voltage, and Table 6 summarizes the corresponding test-voltage and leakage-current values. This descriptive treatment keeps the argument aligned with the available evidence and directly addresses the reviewer concern about over-interpretation.

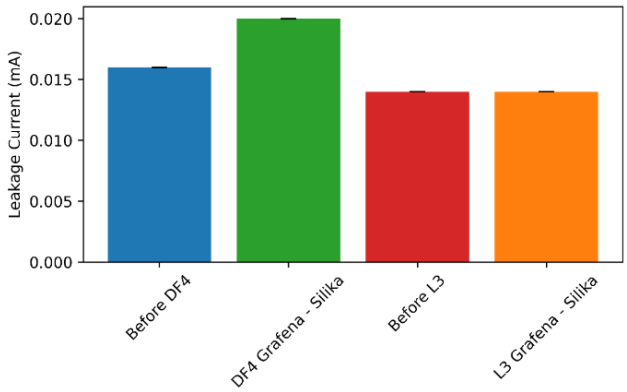

Figure 4. Leakage current of ceramic insulators at 50% flashover voltage before and after SiO_2-graphene coating

The decrease in wet flashover voltage is interpreted as an observed outcome that requires cautious mechanism discussion, not as final proof that the coating is electrically detrimental under all service conditions.

3.6 Electrical field and discharge mechanism interpretation

Under wet contaminated conditions, the insulator surface may contain a discontinuous mixture of droplets, thin films, biological residue, and coated regions. When these regions become electrically connected along a stressed path, local current concentration and dry-band formation can occur even if the static contact angle measured at selected points remains high. Figure 5 illustrates the proposed wet flashover mechanism under contaminated and humid surface conditions.

The proposed mechanism is consistent with the present data, but it should be read as a probable mechanism rather than as a uniquely verified one, because the study did not directly image the evolving wet conductive path during breakdown.

From an engineering perspective, coating development for outdoor insulators should prioritize not only hydrophobicity, but also coverage continuity, durability under biological fouling, and resistance to localized conductive bridge formation.

For field application, these targets are more useful than contact-angle magnitude alone. The discussion therefore distinguishes direct observation, engineering implication, and mechanism inference more clearly.

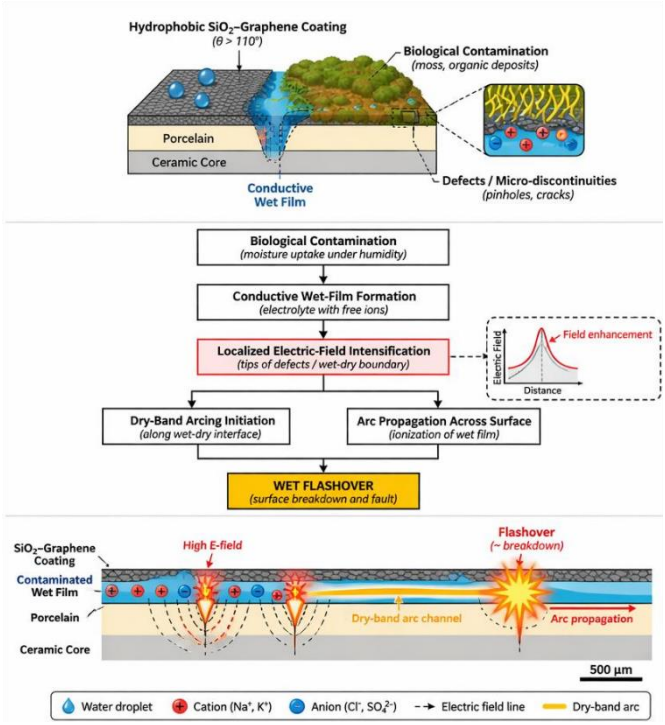

Figure 5. Mechanism of wet flashover

4. CONCLUSION

The results show that SiO_2, graphene, and hybrid SiO_2-graphene coatings increased the measured static contact angle of naturally contaminated 150 kV ceramic insulators, with the hybrid system producing the largest improvement and the lowest post-coating dispersion. FE-SEM, EDS, and FTIR results are consistent with successful surface modification, but the evidence remains qualitative and does not establish a fully quantified morphology-chemistry coupling parameter. Despite the improved wettability, the hybrid-coated specimens did not show higher wet flashover voltage under the studied biological contamination conditions. These findings indicate that static hydrophobicity alone is insufficient to explain wet flashover performance when contamination-assisted conductive paths, local defects, or coating non-uniformity remain present. Within the limits of the available dataset, the main value of this work lies in showing that favorable surface-wetting metrics and adverse wet flashover outcomes can

coexist under natural contamination, which is relevant for the interpretation and qualification of coated outdoor ceramic insulators.

ACKNOWLEDGMENT

This research was financially supported by the Directorate General of Higher Education, Ministry of Education, Culture, Research, and Technology (DIKTI), Indonesia, in collaboration with the National Research and Innovation Agency (BRIN), under Research Contract Numbers 131/C3/DT.05.00/PL/2025, 019/LL10/DT.05.00/PL/2025, and 63/27.O10.1.2/PN/VI/2025. The authors gratefully acknowledge this financial support, which enabled the successful implementation and completion of this research.

REFERENCES

[1] Salem, A.A., Al-Gailani, S.A., Amer, A.A.G., Alsharef, M., Bajaj, M., Zaitsev, I., Ngah, N., Ghoneim, S.S. (2024). Classification of RTV-coated porcelain insulator condition under different profiles and levels of pollution. Scientific Reports, 14(1): 22759. https://doi.org/10.1038/s41598-024-73520-7

[2] Jamaludin, F.A., Chao, C.S. (2024). Effect analysis of pollutant distribution on the flashover performance of porcelain and composite insulator using finite element method. Science & Technology Asia, 29(1): 82-90. https://ph02.tci-thaijo.org/index.php/SciTechAsia/article/view/250691.

[3] Cai, H., Xie, C., Gou, B., Zhou, J., Zhong, A., Zhang, D., Xu, H., Bi, C., Wang, R. (2024). Durable superhydrophobic insulating coatings for prevention of wet flashover and icing in power system. Applied Surface Science, 671: 160768. https://doi.org/10.1016/j.apsusc.2024.160768

[4] Li, C., Dou, P., Zhao, R., Shi, Y., Fu, G., Shen, B. (2023). Preparation and super-hydrophobic mechanism analysis of FAS-17-modified SiO2/PDMS coatings for high-voltage composite insulators. Coatings, 13(3): 563. https://doi.org/10.3390/coatings13030563

[5] Khademsameni, H., Jafari, R., Allahdini, A., Momen, G. (2024). Regenerative superhydrophobic coatings for enhanced performance and durability of high-voltage electrical insulators in cold climates. Materials, 17(7): 1622. https://doi.org/10.3390/ma17071622

[6] Du, B., Chen, N., Mai, Y., Zhang, G., Zhao, Y. (2023). Improving the hydrophobicity and insulation properties of epoxy resins by the self-assembly-induced coating of fluorinated graphene. ACS Applied Materials & Interfaces, 15(27): 32895-32902. https://doi.org/10.1021/acsami.3c04623

[7] Zhang, W., Liu, F., Li, Y., Chen, T., Nwokolo, I.K., Ahmed, S., Han, E.H. (2024). Modified graphene micropillar array superhydrophobic coating with strong anti-icing properties and corrosion resistance. Coatings, 14(3): 247. https://doi.org/10.3390/coatings14030247

[8] Raza, T.A., Kamran, M., Shah, S.A.M., Bashir, M.M. (2025). Wettability's challenge to high-voltage insulators: Polyurethane as preventive coating. Surfaces, 8(2): 40. https://doi.org/10.3390/surfaces8020040

[9] International Electrotechnical Commission. (1984). IEC 587:1984-Methods for evaluating the resistance of insulators to surface pollution. Geneva, Switzerland: IEC.

[10] Wenzel, R.N. (1936). Resistance of solid surfaces to wetting by water. Industrial & Engineering Chemistry, 28(8): 988-994. https://doi.org/10.1021/ie50320a024

[11] Cassie, A.B.D., Baxter, S. (1944). Wettability of porous surfaces. Transactions of the Faraday Society, 40: 546-551. https://doi.org/10.1039/TF9444000546

[12] Quere, D. (2008). Wetting and roughness. Annual Review of Materials Research, 38: 71-99. https://doi.org/10.1146/annurev.matsci.38.060407.132434

[13] Marmur, A. (2008). Concepts and misuses of superhydrophobicity. Langmuir, 24(14): 7573-7579. https://doi.org/10.1021/la801498r

[14] Yarin, A.L. (2006). Drop impact dynamics: Splashing, spreading, receding, bouncing. Annual Review of Fluid Mechanics, 38(1): 159-192. https://doi.org/10.1146/annurev.fluid.38.050304.092144

[15] Farhadi, S., Farzaneh, M., Kulinich, S.A. (2011). Anti-icing performance of superhydrophobic surfaces. Applied Surface Science, 257(14): 6264-6269. https://doi.org/10.1016/j.apsusc.2011.02.057

[16] Zeng, J., Yang, L., Liu, W., Liu, H., Zhang, Y., Li, Z., Liu, X., Chi, X., Cheng, L., Li, S. (2023). Largely enhanced surface flashover voltage of poly(ether imide) by scalable and durable ZnO coating: A gift from in situ growth. ACS Applied Materials & Interfaces, 15(37): 44331-44341. https://doi.org/10.1021/acsami.3c09771

[17] Salem, A.A., Lau, K.Y., Rahiman, W., Al-Gailani, S.A., Abdul-Malek, Z., Abd Rahman, R., Al-Ameri, S.M., Sheikh, U.U. (2021). Pollution flashover characteristics of coated insulators under different profiles of coating damage. Coatings, 11(10): 1194. https://doi.org/10.3390/coatings11101194

[18] Salem, A.A., Lau, K.Y., Abdul-Malek, Z., Al-Gailani, S.A., Tan, C.W. (2022). Flashover voltage of porcelain insulator under various pollution distributions: Experiment and modeling. Electric Power Systems Research, 208: 107867. https://doi.org/10.1016/j.epsr.2022.107867

[19] Salem, A.A., Lau, K.Y., Ishak, M.T., Abdul-Malek, Z., Al-Gailani, S.A., Al-Ameri, S.M., Mohammed, A., Alashbi, A.A.S., Ghoneim, S.S.M. (2022). Monitoring porcelain insulator condition based on leakage current characteristics. Materials, 15(18): 6370. https://doi.org/10.3390/ma15186370

[20] Maraba, L., Al-Soufi, K., Ssenmoga, T., Memon, A.M., Worku, M.Y., Alhems, L.M. (2022). Contamination level monitoring techniques for high-voltage insulators: A review. Energies, 15(20): 7656. https://doi.org/10.3390/en15207656

[21] Kim, T., Yi, J. (2022). Application of hydrophobic coating to reduce leakage current through surface energy control of high voltage insulator. Applied Surface Science, 578: 151820. https://doi.org/10.1016/j.apsusc.2021.151820

[22] Muangpratoom, P., Khonchaiyaphum, I., Vittayakorn, W. (2023). Improvement of the electrical performance of outdoor porcelain insulators by utilization of a novel nano-TiO2 coating for application in railway electrification systems. Energies, 16(1): 561. https://doi.org/10.3390/en16010561

[23] Belhouchet, K., Zemmrit, A., Belhouchet, H., Bayadi, A.,

Romero, M. (2024). Nano-TiO2 coating for improved electrical properties of outdoor high-voltage porcelain insulators. Journal of Materials Science: Materials in Electronics, 35: 1971. https://doi.org/10.1007/s10854-024-13756-1

[24] Ramachandramurthy, P., Yepuni, V. (2025). Hydrophobic TiO2 coatings on porcelain insulators for enhanced surface conductivity and controlled leakage current flow. Transactions on Electrical and Electronic Materials. https://doi.org/10.1007/s42341-025-00665-1

[25] Tong, Z., Bi, M., Zeng, H., Jiang, T., Ma, Z., Zhang, Z. (2026). Study on surface condensation behavior and flashover characteristics of superhydrophobic coating. Journal of Applied Physics, 139(5): 055901. https://doi.org/10.1063/5.0311272